Anisotropy and the approach to scaling in monodisperse reaction-limited cluster-cluster aggregation

1989 J. Phys. A: Math. Gen. 22 1405

(http://iopscience.iop.org/0305-4470/22/9/027)

J. Phys. A: Math. Gen. **22** (1989) 1405-1413. Printed in the UK

Anisotropy and the approach to scaling in monodisperse reaction-limited cluster-cluster aggregation

P B Warren and R C Ball

Cavendish Laboratory, University of Cambridge, Madingley Road, Cambridge, CB3 0HE, UK

Received 4 November 1988

Abstract. We have investigated several models of monodisperse reaction-limited cluster-cluster aggregation in two and three dimensions and have obtained the first systematic theoretical estimations of the overall anisotropy of cluster-cluster aggregates, and the way in which small clusters approach scaling. Our results are supported by simulation and confirm that in the monodisperse case the approach to scaling is very rapid and the clusters are significantly aspherical in aspect ratio.

1. Introduction

General cluster-cluster aggregation occurs when particles, and clusters of particles, move randomly and can stick rigidly together to form larger clusters. The case when the clusters stick on first contact (diffusion-limited case) was the first to be studied (Meakin 1983, Kolb *et al* 1983). Botet *et al* (1984) introduced a simplification by considering monodisperse or hierarchical aggregation in which a set of clusters of equal mass is taken (initially a set of monomers) and the clusters allowed to aggregate in pairs to form a new set. The new clusters are then themselves allowed to aggregate in pairs and so on. This approximation is applicable to cases where the cluster size distribution is approximately monodisperse or the kernel for aggregation in the Smoluchowski equation (von Smoluchowski 1917, see also Ziff *et al* 1985) is strongly biased in favour of the aggregation of clusters of the same size. This model was first introduced by Sutherland (1970) for a slightly different purpose, and has been studied in the diffusion-limited regime by Botet *et al* (1984) and Jullien *et al* (1984).

Kolb and Jullien (1984) allowed the probability of clusters sticking on contact to be less than one. If this probability is small (studied in detail by Meakin and Family (1987)) (there might be a high-energy barrier to sticking, for instance) the clusters come into contact many times before sticking and can explore the entire set of contact configurations without bias. Numerical simulations of this type of aggregation (reaction-limited case) have been studied by Jullien and Kolb (1984) for the monodisperse case and Brown and Ball (1985) for the polydisperse case.

The result of all this numerical simulation has been that the clusters obtained are observed to obey a scaling law consistent with their being fractal objects (Mandelbrot 1982) at least on size scales greater than the individual cluster particle sizes but less

0305-4470/89/091405+09$02.50

than the overall cluster size. The fractal dimensions so obtained depend on which model is used to generate the clusters. For clusters of small size we expect departures from this scaling law. The clusters are not spherical objects but exhibit definite long and short axes.

A model for monodisperse aggregation based on representing the clusters as spheres has been given by Ball and Thompson (1984). This model gives good estimates of the fractal dimensions in both the diffusion-limited and reaction-limited regimes.

The purpose of this paper is to extend the spherical model of Ball and Thompson (1984) to describe the shape of the clusters and to address the problem of the approach to scaling behaviour. In this paper we will consider only monodisperse reaction-limited cluster-cluster aggregation.

Although the spherical model discussed by Ball and Thompson (1984) gives good estimates of the fractal dimension of such clusters, it gives no information on their shape or the approach to scaling behaviour. Their model is essentially a one-parameter model, by introducing more parameters we can get more information out of the model. Not only can we get the expected values of the parameters in the scaling limit, but we can study the approach to scaling—this is achieved by putting different values of the parameters into the model, and observing how they approach the scaling limit. The parameters chosen in this paper are the spans of the clusters along the principal axes of the inertial tensor (in practice, we used the second-moment tensor of the mass distribution, to which the inertial tensor is closely related). We assume that these spans should differ very little from the actual maximum and minimum spans of the clusters. We call these spans a and b in two dimensions, with subscripts if necessary.

Although our model is now richer than the spherical model, we will still have to make severe approximations to force 'closure', to relate aggregates back to the original description. The first approximation we make is on the set of clusters of a given mass. There will in general be a distribution of spans in this set, and we are taking a particular pair of values (a, b) for the spans as representative of the set (this approximation is also present in the spherical model). We apply the same approximation for the inertial tensor. The set of clusters is represented by these spans and this inertial tensor, which we can envisage as an ellipse (although we really only use the spans of such an ellipse). Note that the inertial tensor is not equivalent to the inertial tensor of a solid ellipse of the same spans because the internal mass distribution is not uniform.

We model the aggregation process by sticking two ellipses together. The problem now is that there are many different configurations of mutual contact for two ellipses. This problem is not present in the spherical model since there is only one way to stick two discs together. The different configurations give rise to different spans of the resulting object—there is a distribution of spans over the set of mutual configurations and we are required to pick two values for the spans as being representative of this distribution, in order to be consistent with the first approximation discussed above.

Our next approximations are to pick out a subset of this set of configurations for consideration, decide what relative weighting to give to the different configurations, and finally find a pair of values (a, b) representative of the distribution of spans. The many different ways of doing this give rise to many different models, two of which are outlined below.

The new pair of spans for the aggregate object are, in all but the simplest cases, non-linear functions of the spans of the original ellipses. These constitute recurrence relations for the cluster parameters. We can both extract the limiting scaling behaviour and quantify the approach to scaling from these.

2. T model: modal configuration

The modal configuration in two dimensions, i.e. that having the greatest relative weighting, was considered to be that in which the long axis of one ellipse abuts against the short axis of the other ellipse in a T configuration (figure 1). The weight of such a configuration is certainly a local maximum—the spans of the object do not depend on slight variations away from the T configuration. The T model uses only this modal configuration in the calculation, and as a consequence is simple and linear.

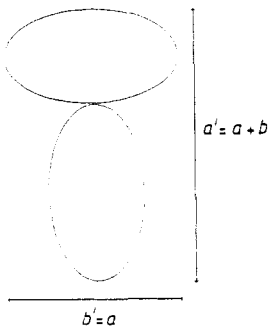

Figure 1. The T model: the modal configuration for two ellipses in mutual contact in $d = 2$.

If the two original ellipses have spans a and b, then the T object will have spans a' and b' given by

$$a' = a + b \qquad b' = a$$

or, in matrix form,

$$\begin{bmatrix} a \\ b \end{bmatrix}' = \begin{bmatrix} 1 & 1 \\ 1 & 0 \end{bmatrix} \begin{bmatrix} a \\ b \end{bmatrix}.$$

In the scaling limit we require the new object to be simply a scaled version of the original, i.e. $a'/a = b'/b$. This is equivalent to finding the eigenvalues and eigenvectors of the matrix (choosing the sensible ones).

This allows us to calculate the fractal dimension (from the eigenvalue) and the shape (from the eigenvector):

$$D_F = \ln 2 / \ln \tau \qquad a/b = \tau$$

where τ = golden mean $= \frac{1}{2}(1+\sqrt{5})$.

By introducing the radii of gyration about the long and short principal axes to characterise the inertial tensor, we can calculate their expected ratio in the scaling limit. This ratio turns out to be different from the ratio a/b:

$$R_L / R_S = \tau^{3/2}.$$

The actual values of these parameters are collected in table 1.

The approach to scaling can be analysed, and is seen to depend on that eigenvalue of the matrix which was not used for the fractal dimension. The leading correction to scaling is contained in the following formula for the long span:

$$a \sim M^{1/D}(1 \pm kM^{-\theta} + \ldots) \tag{1}$$

Table 1. Data for cluster aggregation in two dimensions. The computer simulation and models are discussed in the text. A figure in brackets after a result is an estimate of the error in the final digit of that result. The parameters refer to fractal dimension (D_F), cluster span ratio (a/b), ratio of radii of gyration (R_L/R_S), and approach to scaling (θ, ϕ; see equation (2) in the text).

$d=2$	D_F	a/b	R_L/R_S	θ	ϕ
Computer simulation	1.55 (1)	1.78 (2)	2.23 (2)	0.7–1.6	
T model	1.44	1.62	2.06	1.39	$\pi/\log 2$
Averaged model	1.54	1.76	1.98	2.30	$\pi/\log 2$

where $\theta = 2\log\tau/\log 2 = 2/D_F$. A similar result is obtained for b. The sign of the correction alternates with each cycle of the aggregation process. In the particular case of the T model in two dimensions, the leading-order correction is the only correction term to a and b, and (1) is exact.

We can rewrite the correction formula (1) in the following way:

$$a \sim M^{1/D}[1 + kM^{-\theta}\cos(\phi \log M - \phi_0) + \ldots] \tag{2}$$

where $\phi = \pi/\log 2$ and ϕ_0 is an uninteresting constant. The reason for this more complicated formula will become obvious when we discuss the modal configuration in three dimensions, where a non-trivial value of ϕ occurs. The values of θ and ϕ are given in table 1 and the theoretical behaviour is shown in figure 3. Our large value of θ implies a very rapid approach to scaling, consistent with the success of relatively small simulations in reproducing the scaling of large experimental clusters.

The correction terms for the radii of gyration are complicated by the initial values given to the monomers. Unless these are matched to the initial spans of the monomers, there will be a constant term in the inertial tensor, giving rise to a correction term showing straightforward decay (no oscillations) with $\theta = 2/D$. If the constant is dropped, the leading term coming purely from the model is an oscillating correction, having the same value of θ (namely $2/D$).

In our simulations we studied the ratio a/b, since this is expected to go to a constant, with the same leading-order correction as a and b individually. It is easier to extract the approach to scaling from the computer data when the quantity being considered tends to a constant. It is still, however, very difficult in practice to measure θ and ϕ.

3. Averaged model

An obvious generalisation of the T model which is still mathematically tractable is to consider the subset of configurations where any axis of the first ellipse abuts against any axis of the second. In the absence of evidence to the contrary, we weight each configuration equally. It should be emphasised that such a weighting is still an arbitrary choice, however. When all the degeneracies are counted, we are left with three distinct configurations of which the T carries twice the weight of the other two (figure 2). A complication arises for the configuration in which the two short axes are in contact (configuration A in figure 2), in that the spans of the resulting object 'cross over' as the ratio a/b of the spans of the original ellipses is increased past the value two. To

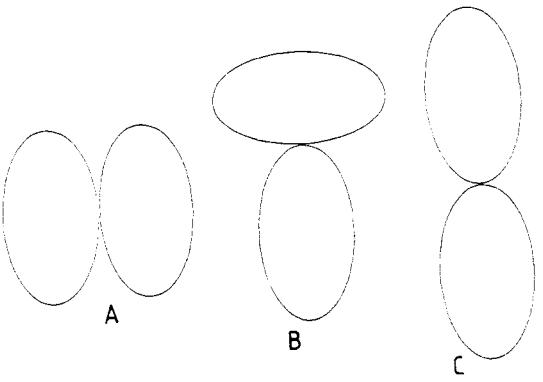

Figure 2. The three configurations in the averaged model. The relative weights of A, B and C are 1:2:1.

Table 2. Data for cluster aggregation in three dimensions. The computer simulation and models are discussed in the text. A figure in brackets after a result is an estimate of the error in the final digit of that result. The parameters refer to fractal dimension (D_F), cluster span ratios (a/c, b/c), and approach to scaling (θ, ϕ; see equation (2) in the text).

$d=3$	D_F	a/c	b/c	θ	ϕ
Computer simulation	1.97 (2)	2.11 (2)	1.38 (2)	0.7–1.9	
Modal configuration	1.81	2.15	1.47	0.83	1.29
Averaged model	1.90	2.06	1.37	2.86	$\pi/\log 2$

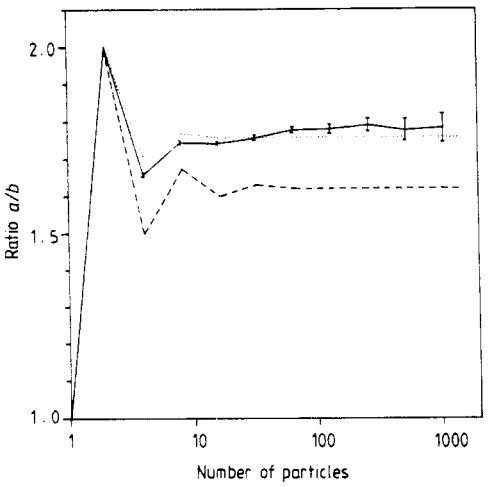

Figure 3. Cluster span ratio a/b against number of particles in two dimensions. The simulation consisted of 102 400 particles aggregated on a square lattice to form 100 clusters of 1024 particles. The error bars are *one* standard deviation. The two models are discussed in the text. The full curve represents the results of the computer simulation, the broken curve represents the T model and the dotted curve represents the averaged model.

conform with our implicit requirement that $a' > b'$ (given $a > b$) we divide the a/b line into two intervals $(1, 2)$ and $(2, \infty)$. This means the model is non-linear.

We take the new overall spans to be a straightforward average of the spans of the composite objects, with the weighting indicated previously. Note that since we are really only concerned with the ratio of spans, we could average over the ratios of spans, rather than find the ratio of the average spans. This amounts to choosing different fundamental parameters in the model—namely one span, and the aspect ratio. There is no objection to this, but for simplicity we remain with the spans, and use the ratio of the averages. For consistency, the data from the computer simulation was also a ratio of averages.

Performing an analysis similar to that for the T model, and averaging, we obtain a different matrix for each interval. Fortunately, when we calculate the ratio a/b from the eigenvectors of each matrix, only one lies in its own interval on the a/b line, so we can unambiguously choose that limit point to the scaling behaviour. The results of the calculations are shown in table 1.

In the approach to scaling, for small deviations, we can use the other eigenvalue of the matrix corresponding to the stable limit point to calculate the leading correction term, which turns out to be similar to that for the T model and is shown in table 2. For large deviations the non-linearity of the model admits of no simple result, but we can consider individual cases. The behaviour starting from monomers of equal spans is shown in figure 3.

4. Three-dimensional models

The model is easily extended to three dimensions—the set of clusters is modelled by an ellipsoid with three spans, a, b and c, along the three principal axes.

There are twelve distinct ways of joining two ellipsoids so that their principal axes are parallel, and the contact point lies on an axis of both ellipsoids. Six of these configurations have twice the weight as the others; however, two of the six give rise to the same spans of the composite object, so this can be considered to be the modal configuration.

Doing an analysis for each distinct configuration, we find many instances where the spans 'cross over' and we treat these in the same way as the two-dimensional model. Averaging as before, we find that the $(a/c, b/c)$ plane is divided into seven separate regions, with a different matrix for each (figure 4). Remarkably, when the limit points $(a/c, b/c)$ are calculated from the eigenvectors of the matrices, only one is found to lie in its own region. This was taken to be the limit point for the model. The results for the fractal dimension and ratio of spans are set out in table 2.

The modal configuration mentioned above corresponds to the shortest axis of one ellipsoid abutting against the longest axis of the other. There are then two possible orientations of the second ellipse relative to the first (their middle length axes can run parallel or perpendicular) but the spans of the composite object are the same for both. This configuration is the analogue of the T in two dimensions. The results for the fractal dimension and ratio of spans, using this modal configuration alone, are shown in table 2.

The approach to scaling is calculated in the same way as in two dimensions. In the averaged model, for small deviations, the leading-order correction comes from the second-largest eigenvalue (the fractal dimension comes from the largest), and exhibits

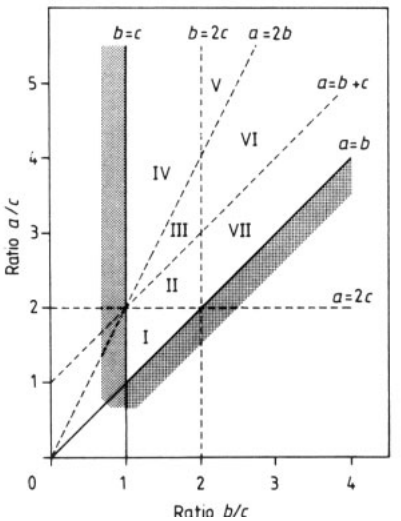

Figure 4. The $(a/c, b/c)$ plane is divided into seven separate regions in the averaged model. There is a different matrix in each region relating the spans of the new object to the spans of the old, but only the matrix in region II has a limit point lying on its own region. Note that values in the plane are restricted to a wedge by the convention $a \geqslant b \geqslant c$.

oscillating decay like the two-dimensional models. The general behaviour for large deviations is complex because of the non-linear nature of the model, but can be easily calculated for specific cases. In the modal configuration, the matrix has two second-largest eigenvalues, which are complex conjugates (the matrix is real but non-symmetric). This leads to a non-trivial value for ϕ in (2) so (2) is now exact since all three eigenvalues have been used. The values of θ and ϕ for both models are collected in table 2 and the theoretical curves, starting from monomers of equal spans, are shown in figure 5. The small value of θ for the modal configuration, and the non-trivial value of ϕ are responsible for the relatively wild behaviour of the theoretical curve of the modal configuration.

5. Computer simulations

In two dimensions several computer simulations were performed on both square and hexagonal lattices, the largest of which involved aggregating 102 400 particles to form 100 clusters of size 1024 particles. The results were collated and are compared with those of the models in table 1. As can be seen, the comparison is good, although the averaged model performs better than the T model. The results from the hexagonal lattice simulation were found to agree with those from the square lattice simulation for cluster sizes greater than four particles. The data for the approach to scaling of the ratio of spans a/b is plotted in figure 3, alongside the theoretical predictions of the models.

In three dimensions computer simulations on a simple cubic lattice were performed, also involving a run of 102 400 particles aggregating to form 100 clusters of size 1024. The results are in table 2 for comparison with the results of the three-dimensional models described above. The results of the averaged model compare well with the

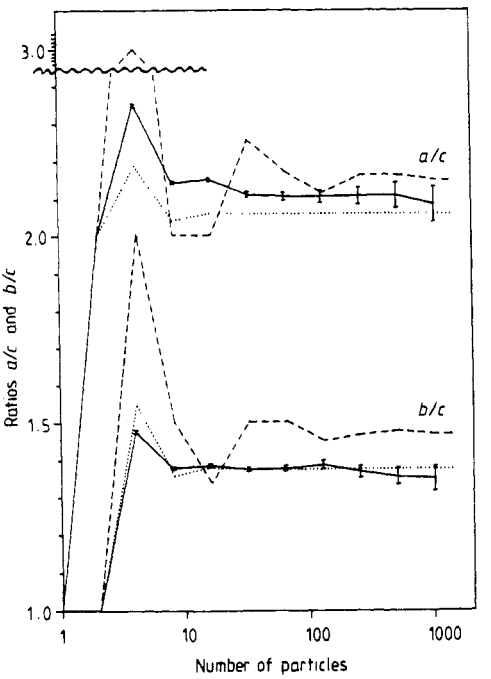

Figure 5. Cluster span ratios a/c and b/c against number of particles in three dimensions. The simulation consisted of 102 400 particles aggregated on a simple cubic lattice to form 100 clusters of 1024 particles. The error bars are *one* standard deviation. The upper curves are for the ratio a/c and the lower for b/c. The models are discussed in the text. The full curve represents the results of the computer simulation, the broken curve represents the modal configuration, and the dotted curve represents the averaged model.

computer simulation; those of the modal configuration are not as good. The data for the ratios of spans a/c and b/c showing the approach to scaling is plotted in figure 5, again with the theoretical predictions.

If we assume that (2) provides a valid description of the approach to scaling we could measure the values of θ and ϕ from the simulation data. In practice we could only extract an approximate range for θ. It proved too difficult to measure ϕ from the available data, but qualitatively there appears to be some evidence of oscillations in both $d = 2$ and $d = 3$ suggesting ϕ has a value near $\pi/\log 2$.

On a technical note, the aggregation was performed by producing a list of surface sites of one cluster, then placing a particle of the second cluster in a surface site and accepting the configuration if the clusters do not overlap. The alternative is to repeatedly place the clusters close together (in a box, for example) and accept the first configuration in which the clusters are in contact but not overlapping. The difference between the two methods lies in configurations with multiple contacts. Such a configuration can be generated in several ways by the first method, but in only one way by the second. The probability of obtaining such configurations is enhanced in proportion to the number of contacts by using the surface-sites method, which seems closer to physical reality. However, the difference between the two methods does not appear to have much influence on the scaling properties (Kolb and Jullien 1984, Meakin and Family 1987). An advantage of the surface-sites method is that it is easier to go off lattice than the random-position method.

6. Conclusions

We have described several models which are extensions of the spherical model of Ball and Thompson (1984) and which describe monodisperse reaction-limited cluster-cluster aggregation. The models predict fractal dimensions and cluster span ratios which agree quite well with data from numerical simulations. We are also able to extract information on the approach to scaling and this suggests a more general form for the approach to scaling might be relevant, involving oscillations of the leading-order corrections as well as a power-law decay with increasing cluster mass. Although it has proved difficult to quantify the approach to scaling for real clusters formed in the simulations, there is, however, a broad agreement between the models and the simulation data. Future work will involve finer testing of the assumptions in the models, particularly the rather *ad hoc* weighting given to configurations in the averaged models, performing numerical simulations off lattice and extending the models to describe polydisperse aggregation.

References

Ball R C and Thompson B R 1984 *J. Phys. A: Math. Gen.* **17** L951
Botet R, Jullien R and Kolb M 1984 *J. Phys. A: Math. Gen.* **17** L75
Brown W D and Ball R C 1985 *J. Phys. A: Math. Gen.* **18** L517
Jullien R and Kolb M 1984 *J. Phys. A: Math. Gen.* **17** L639
Jullien R, Kolb M and Botet R 1984 *J. Physique Lett.* **45** L211
Kolb M, Botet R and Jullien R 1983 *Phys. Rev. Lett.* **51** 1123
Kolb M and Jullien R 1984 *J. Physique Lett.* **45** L977
Mandelbrot B B 1982 *The Fractal Geometry of Nature* (San Francisco: Freeman)
Meakin P 1983 *Phys. Rev. Lett.* **51** 1119
Meakin P and Family F 1987 *Phys. Rev.* A **36** 5498
Sutherland D N 1970 *Nature* **226** 1241
von Smoluchowski M 1917 *Z. Phys. Chem.* **92** 129
Ziff R M, McGrady E D and Meakin P 1985 *J. Chem. Phys.* **82** 5269